

## SEDIMENTATION OF TWO SPHERES IN A SQUARE TUBE

by

**Geng GUAN, Yuxiang YING, and Deming NIE\***

Institute of Fluid Mechanics, China Jiliang University,  
Hangzhou, Zhejiang, China

Original scientific paper  
<https://doi.org/10.2298/TSCI21S2373G>

*In this study, we simulated the sedimentation of two identical spheres having the same density in a square tube. Compared with the center-line and the diagonal planes (including the reverse diagonal plane), the sedimentation of spheres on other planes is more complicated. Results show that at relatively low and high Reynolds number, the spheres will deflect and eventually move to the diagonal plane of the square tube. At the medium Reynolds number, the spheres settle near the initial plane. The possible mechanisms underlying these behaviors are examined. Finally, it is shown that the distance between the spheres increases with an increase in the Reynolds number, which is applicable to all the initial settlement planes studied.*

Key words: *sedimentation, Reynolds number, center-line plane*

### Introduction

Multiple particles in a fluid generate hydrodynamic interactions, which will have a tremendous effect on the movement of particles and the overall properties of the suspension under the inertial force of the particles and the fluid. Because of its simplicity and convenience, 2-D flow has always been favored by researchers. The drifting-kissing-tumbling Fortes *et al.* [1] phenomenon has been revealed through the finite element method [2]. Other studies have examined the effect of particle size, Wang *et al.* [3], Reynolds number, Nie *et al.* [4], array mode, Yacoubi *et al.* [5] the distances between particles, and Nie *et al.* [6] on particle sedimentation.

Regarding the 3-D aspects of the settlement system, previous research has focused on the movement patterns of particles [7, 8] and the wall effect, Luo *et al.* [9] when they settle. It is worth noting that particles have different stable settlement planes under different Galileo numbers, Nie *et al.* [10], a topic that has inspired our research. The purpose of our study is to provide a comprehensive understanding of the interaction of two-particle sedimentation in a square tube.

### Lattice Boltzmann method

In this work, 3-D lattice Boltzmann method (LBM) is employed. The discrete lattice Boltzmann equation of the single-relaxation time model is:

$$f_i(\mathbf{x} + \mathbf{e}_i \Delta t, t + \Delta t) - f_i(\mathbf{x}, t) = -\frac{1}{\tau} [f_i(\mathbf{x}, t) - f_i^{(0)}(\mathbf{x}, t)] \quad (1)$$

\* Corresponding author, e-mail: nieinhz@cjlu.edu.cn

where  $f_i(\mathbf{x}, t)$  is the distribution function of the microscopic velocity,  $e_i$ , in the  $i^{\text{th}}$  direction,  $f_i^{(0)}(\mathbf{x}, t)$  – the equilibrium distribution function,  $\Delta t$  – the time step of the simulation, and  $\tau$  – the relaxation time and is related to the fluid viscosity,  $\nu$ .

The density and velocity of fluid are computed:

$$\rho = \sum_i f_i, \quad \rho \mathbf{u} = \sum_i f_i \mathbf{e}_i \quad (2)$$

For the 3-D particle settlement simulation, the 19-velocity (D3Q19) lattice model is used. The discrete velocity vector is:

$$\mathbf{e}_i = \begin{cases} (0, 0, 0)c & i = 0, \\ (\pm 1, 0, 0)c, (0, \pm 1, 0), (0, 0, \pm 1)c & i = 1-6 \\ (\pm 1, \pm 1, 0)c, (\pm 1, 0, \pm 1)c, (0, \pm 1, \pm 1)c & i = 7-18 \end{cases} \quad (3)$$

The equilibrium distribution function  $f_i^{(0)}(\mathbf{x}, t)$  is defined by:

$$f_i^{(0)}(\mathbf{x}, t) = w_i \rho \left[ 1 + \frac{3\mathbf{e}_i \cdot \mathbf{u}}{c^2} + \frac{9(\mathbf{e}_i \cdot \mathbf{u})^2}{2c^4} - \frac{3\mathbf{u} \cdot \mathbf{u}^2}{2c^2} \right] \quad (4)$$

where  $c = \Delta x / \Delta t$ , in which  $\Delta x$  is the lattice separation distance. The speed of sound is related to  $c_s^2 = c^2/3$ , and the weights are set as  $w_0 = 1/3$ ,  $w_{1-6} = 1/18$ , and  $w_{7-18} = 1/36$ .

For the convenience of calculation, the lattice grid,  $\Delta x$ , and time step,  $\Delta t$ , are both fixed at 1, settings adopted in most lattice Boltzmann simulations. In addition, an interpolation-based bounce-back scheme is employed to treat the curved boundaries of solid particles, Lallemand *et al.* [11]. To account for the lubrication effects between particles at small distances, a lubrication force model is also introduced, Nguyen *et al.* [12].

### Problem description

In this work, we study the settlement motion of two interacting spheres in a square tube. The computational model is shown in fig. 1(a). Two spheres are released at rest in a square tube containing a fluid with a density,  $\rho$ , and a kinematic viscosity,  $\nu$ . The diameter and density of these two spheres are expressed as  $d$  and  $\rho_s$ , respectively. The tube width,  $L$ , is  $5d$  with a height,  $H$ , of  $25d$ . The center-line, diagonal, and reverse diagonal planes of the square tube are marked in fig. 1(b). We use a movement field to mimic an infinite tube. Nonslip boundary conditions are applied to all the walls of the tube. At the upper and bottom boundaries, the normal derivative of the velocity is 0.

Because of the unpredictability of the final velocities of particles, the velocity scale is placed at:

$$U_0 = \sqrt{\left(\frac{\rho_s}{\rho} - 1\right)gd} \quad (5)$$

where  $g$  is the gravitational acceleration, which is fixed at  $g = 9.8 \times 10^{-4}$ . The density of the fluid and the two spheres are fixed at  $\rho = 1$ ,  $\rho_s = 1.5$ . The diameters of the two spheres are fixed at  $d = 20$ . The time scale is fixed at  $T_0 = d/U_0$ . In addition, all parameters are lattice parameters. Spheres 0 and 1 are used to distinguish these two identical spheres. Before releasing the spheres under gravity, they are placed as shown in fig. 1(b). In fig. 1(b),  $D_0 = 2d$ , where  $D_0$  is the

distance between the centers of the two spheres, Note that  $\theta_0$  is the angle between the initial and center-line planes, which has four values of  $5^\circ$ ,  $15^\circ$ ,  $25^\circ$ , and  $35^\circ$ . In the simulation, the initial positions of Spheres 0 and 1 are determined by the angle  $\theta_0$ .

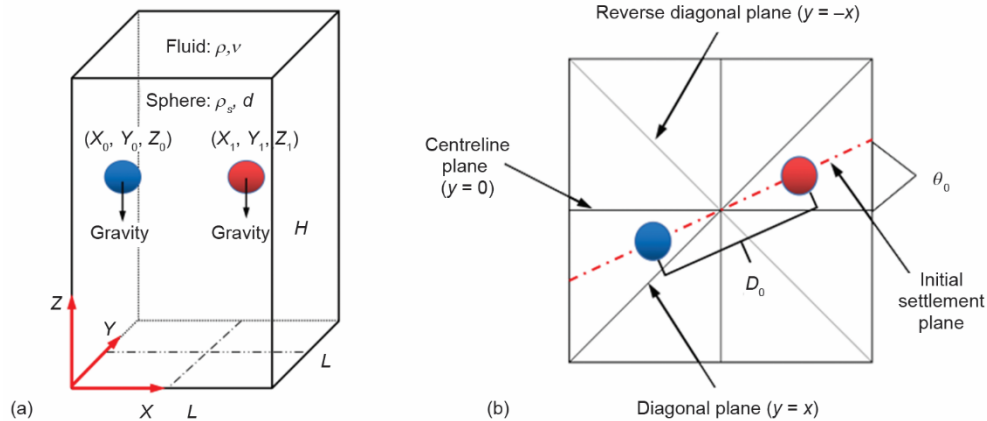


Figure 1. Diagrammatic description of two spheres of sedimentation in a square tube

### Numerical results

In the simulation, when the particle sedimentation was fully developed, the particles eventually reached steady-state sedimentation on a single plane. To illustrate more effectively the situation of particle sedimentation in the square tube, we used different Reynolds numbers ( $Re = 20, 60, 120,$  and  $140$ ) at  $\theta_0 = 5^\circ$  to present the particle trajectories after steady-state sedimentation, as shown in fig. 2.

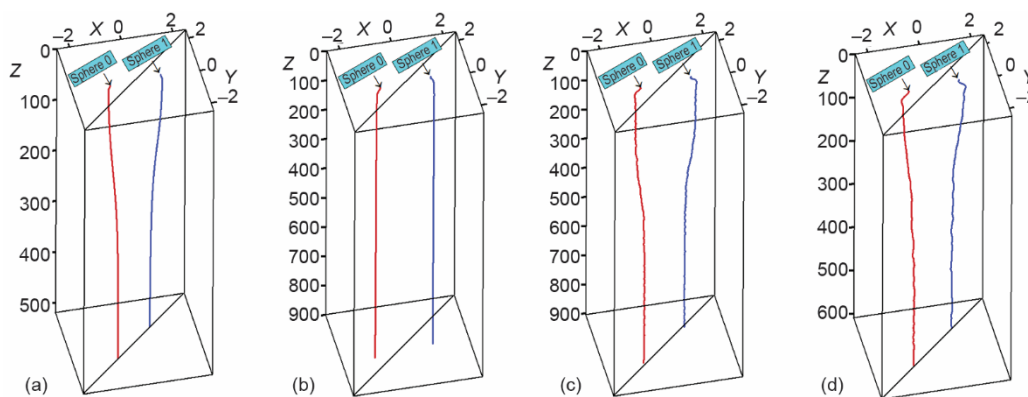


Figure 2. Trajectories of the spheres for  $\theta_0 = 5^\circ$ ; (a)  $Re = 20$ , (b)  $Re = 60$ , (c)  $Re = 120$ , and (d)  $Re = 140$

Figure 2(a) presents the trajectories of the two spheres for  $\theta_0 = 5^\circ$  at  $Re = 20$ , where it can be observed that the two spheres first repelled each other, and then began to leave the initial plane. A period then passed before they moved to the diagonal plane. Nevertheless, the spheres may remain at the initial settlement plane at a relatively medium Reynolds number value, and fig. 2(b) shows the trajectories of the two spheres for  $\theta_0 = 5^\circ$  at  $Re = 60$ . Different behaviors were observed, namely, the spheres did not seem to leave the initial plane after repelling each other. When the Reynolds number reached relatively high values, such as

Re = 120 and 140, as shown in figs. 2(c) and 2(d), respectively, the same movement as that of a lower Reynolds number reappeared.

Figure 3 shows the 3-D structure of the flow field around the particles after stable settlement for  $\theta_0 = 5^\circ$  at Re = 120. The vortical structure presented in fig. 3 was proposed by Jeong and Hussain [13], who considered the tensor  $\mathbf{S}^2 + \mathbf{\Omega}^2$  to determine whether there was a local pressure minimum derived from vortical motion, where  $\mathbf{S}$  and  $\mathbf{\Omega}$  are the symmetrical and anti-symmetrical parts of the velocity gradient tensor, respectively. Because of the symmetry of  $\mathbf{S}^2 + \mathbf{\Omega}^2$ , only real eigenvalues exist for  $\mathbf{S}^2 + \mathbf{\Omega}^2$ . In addition the vortical structures are identified by  $\lambda_2 < 0$  within the vortex core, where  $\lambda_2$  is the second largest eigenvalue of  $\mathbf{S}^2 + \mathbf{\Omega}^2$ . Figure 3 shows that, in our study, the vortex motion was concentrated in the thin torus-area surrounding the spheres.

Here, the parameter  $\delta$  was introduced to describe the effect of  $\theta_0$  on particle settlement, where  $\delta$  is determined by  $\delta = (\theta_1 - \theta_0)/(45^\circ - \theta_0)$  to describe the deflection rate of particles, and  $\theta_1$  represents the angle between the steady settlement and center planes. The result is shown in fig. 4, where the effects of  $\theta_0$  on different Reynolds number values were different. It was observed that the value of  $\theta_0$  had little effect on the  $\delta$  of particles when Reynolds number was relatively high or low, as shown in fig. 4. However, the  $\delta$  of particles was more dependent on the value of  $\theta_0$  at a relatively moderate Reynolds number. For example, large fluctuations could not be observed when Re = 20, 40, and 120 but appeared at Re = 60, 80, and 100.

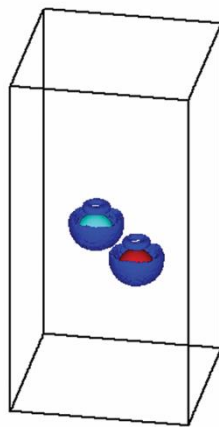


Figure 3. Reference results for  $\theta_0 = 5^\circ$  (Re = 120), the surface where  $\lambda_2 = -0.0004$

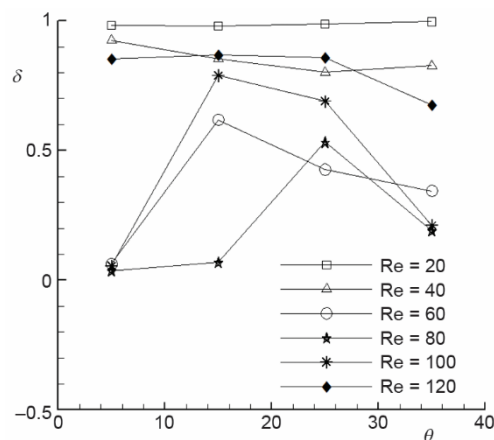
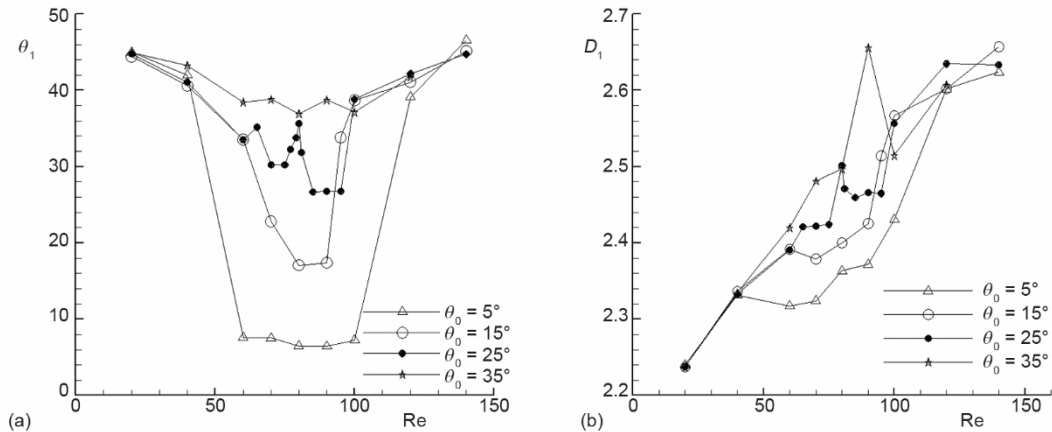


Figure 4. Deflection rate,  $\delta$ , of particles with  $\theta_0 = 5^\circ, 15^\circ, 25^\circ$ , and  $35^\circ$  at different Reynolds number

To examine further settlement behavior of the particles in the tube, we observed angle  $\theta_1$ , which was affected by  $\theta_0$  and Reynolds number. Figure 5(a) shows the corresponding results for  $\theta_0 = 5^\circ, 15^\circ, 25^\circ$ , and  $35^\circ$  at different Reynolds number values. As fig. 5(a) indicates, for all  $\theta_0$ ,  $\theta_1$  showed a trend of first declining and then increasing. However we observed that an abnormal increase occurred in the curve shown in fig. 5(a) at Re = 70-90 for  $\theta_0 = 25^\circ$  and also at Re = 80-100 for  $\theta_0 = 35^\circ$ , which were different from the results of  $\theta_0$  at lower values. This was because the larger the  $\theta_0$ , the closer were the spheres to the diagonal plane of the tube, and lower was the wall effect caused by the tube. As fig. 5(b) shows,  $D_1$  is defined as  $D_1 = D_0/d$ , where  $D_1$  represents the spacing between the two spheres at the time of stable settlement. The effect of Reynolds number on  $D_1$  was significant, and  $D_1$  increased as Reynolds number increased. In

addition, a difference in  $D_1$  could still be observed between the larger and smaller  $\theta_0$ . As fig. 5(b) indicates,  $D_1$  abruptly increased when  $Re = 70-90$  for  $\theta_0 = 25^\circ$  and also abruptly increased when  $Re = 80-100$  for  $\theta_0 = 35^\circ$ , which was consistent with  $\theta_1$ .



**Figure 5. Angle,  $\theta_1$ , and distance of the two spheres for different  $Re = 20-140$**

The instantaneous pressure distributions in the top view plane are presented to examine the motion pattern of the spheres for  $\theta_0 = 25^\circ$  at  $Re = 70, 80,$  and  $90$ , when they were stable. As fig. 6 shows, a high pressure area could be observed at the opposite corner of the square tube, which created a strong repulsive force and caused the spheres to approach the diagonal plane. As both spheres–spheres or spheres–walls had a higher pressure at  $Re = 80$ , a higher  $\theta_1$  existed when  $Re = 80$ , which caused the pressure between the spheres and walls to increase. In addition, because the pressure between the spheres was greater, the distance between the spheres was greater, which corresponded to the result shown in fig. 5. Because of the hydrodynamic interaction, the spheres were forced to leave the initial settlement plane. Therefore the initial settlement plane was not a stable settlement plane for the spheres in our study.

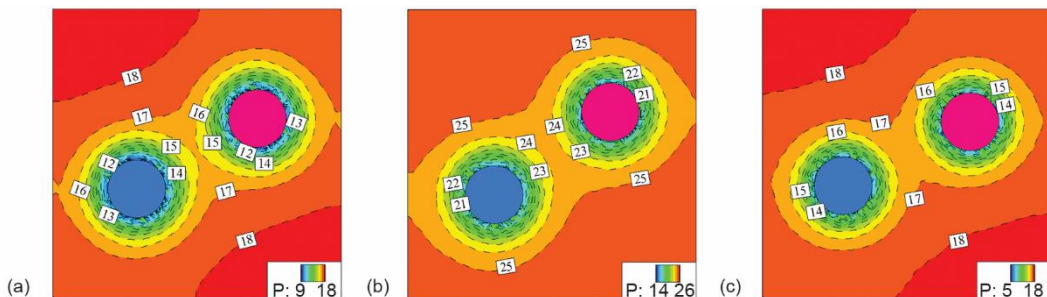


**Figure 6. Instantaneous pressure distributions (top view) when the settlement is stable at  $\theta_0 = 25^\circ$ ; (a)  $Re = 70$ , (b)  $Re = 80$ , and (c)  $Re = 90$**

**Conclusion**

In our work, a 3-D LBM was adopted to simulate the sedimentation of two identical spheres in a square tube. The two resting spheres were released in the initial plane. The effects of the angle,  $\theta_0$ , of the initial settlement plane and different Reynolds numbers, on the stable

sedimentation plane were studied. The results of a lower  $\theta_0$  ( $\theta_0 = 5^\circ$  and  $\theta_0 = 15^\circ$ ) showed a strong regularity. However, a more complex sedimentation regularity occurred at a higher  $\theta_0$  ( $\theta_0 = 25^\circ$  and  $\theta_0 = 35^\circ$ ) because of the lower effect of the wall. The results also indicated that at lower or higher Reynolds number ( $Re \leq 40$  or  $Re \geq 120$ ) the two spheres always reached stable sedimentation at the diagonal plane, irrespective of their initial settlement  $\theta_0$ . However at a medium Reynolds number, the spheres settled near the initial plane.

### Acknowledgement

This work was supported by the National Natural Science Foundation of China (Grant No. 12132015, 11632016, and 11972336)

### Reference

- [1] Fortes, A. F., et al., Non-linear Mechanics of Fluidization of Beds of Spherical Particles, *Journal of Fluid Mechanics*, 177 (1987), Apr., pp. 467-483
- [2] Feng, J., et al., Direct Simulation of Initial Value Problems for The Motion of Solid Bodies in A Newtonian Fluid Part 1 sedimentation, *Journal of Fluid Mechanics*, 261 (1994), 2, pp. 95-134
- [3] Wang, L., et al., Drafting, Kissing and Tumbling Process of Two Particles with Different Sizes, *Computer & Fluids*, 96 (2014), June, pp. 20-34
- [4] Nie, D. M., et al., Grouping Behavior of Coaxial Settling Particles in A Narrow Channel, *Physical Review E*, 93 (2016), 1, ID 013114
- [5] Yacoubi, A. E., et al., Computational Study of the Interaction of Freely Moving Particles At Intermediate Reynolds Numbers, *Journal of Fluid Mechanics*, 705 (2012), July, pp. 134-148
- [6] Nie, D. M., et al., Direct Numerical Simulation of Multiple Particles Sedimentation at An Intermediate Reynolds Number, *Communications in Computational Physics*, 16 (2014), 3, pp. 675-698
- [7] Cao, C., et al., Simulating the Interactions of Two Freely Settling Spherical Particles in Newtonian Fluid Using Lattice-Boltzmann Method, *Applied Mathematics and Computation*, 250 (2015), Jan., pp. 533-551
- [8] Chen, R. Q., Nie, D. M., Kinetic Analysis of the Settlement of Double Particles, *Computational Mechanics*, 33 (2016), 6, pp. 895-94
- [9] Luo, K., et al., Fully-Resolved DNS Study of Rotation Behaviors of One and Two Particles Settling Near a Vertical Wall, *Powder Technology*, 245 (2013), 8, pp. 115-125
- [10] Nie, D. M., Lin, J. Z., Simulation of Sedimentation of Two Spheres with Different Densities in a Square Tube, *Journal of Fluid Mechanics*, 896 (2020), Aug., A12
- [11] Lallemand, P., Luo, L. S., Lattice Boltzmann Method for Moving Boundaries, *Journal of Computational Physics*, 184 (2003), 2, pp. 406-421
- [12] Nguyen, N. Q., Ladd, A. J. C., Lubrication Corrections for Lattice-Boltzmann Simulations of Particle Suspensions, *Physical Review E*, 66 (2002), 4, ID 046708
- [13] Jeong, J., Hussain F., On the Identification of a Vortex, *Journal of Fluid Mechanics*, 285 (1995), Feb., pp. 69-94